Nanoscale

RSC Publishing

PAPER

View Article Online
View Journal | View Issue

Multi-walled carbon nanotube-based carbon/carbon composites with three-dimensional network structures†

Cite this: *Nanoscale*, 2013, **5**, 6181

Yuguang Jin,[a] Yingying Zhang,*[b] Qiang Zhang,[a] Rufan Zhang,[a] Peng Li,[a] Weizhong Qian[a] and Fei Wei*[ab]

Multi-walled carbon nanotube (MWCNT)-based carbon/carbon composites were fabricated by the chemical vapor infiltration of pyrolytic carbon into pre-compressed MWCNT blocks. The pyrolytic carbon was deposited on the surface of the MWCNTs and filled the gaps between the MWCNTs, which improved the connection between the MWCNTs and formed a three-dimensional network structure. The mechanical and electrical properties were improved significantly. The values of the maximum compressed deformation, maximum breaking strength, Young's modulus and energy absorption are measured as 10.9%, 148.6 MPa, 1588.6 MPa and 13.8 kJ kg^{-1}, respectively. The conductivity reached about 204.4 S cm^{-1}, more than 10 times larger than that of pre-compressed MWCNT blocks. After annealing at 1800 °C in vacuum, the graphitization improved remarkably. The pyrolytic carbon deposited on the surface of the MWCNTs was rearranged along the walls, and resulted in an increase of the number of walls of the MWCNTs.

Received 1st March 2013
Accepted 8th May 2013

DOI: 10.1039/c3nr01069d

www.rsc.org/nanoscale

Introduction

Carbon/carbon (C/C) composites have been extensively investigated as a family of advanced composite materials due to their prominent properties, such as low density, high thermal conductivity, and excellent mechanical properties at high temperature.[1,2] Many applications of C/C composites in the field of aerospace including rocket nozzles, exhaust cones, re-entry nose tips and replacement components of metallic brake systems for aircraft disk-brakes have been realized.[1,2] Generally, C/C composites consist of a carbon matrix reinforced by carbon fibers (CFs), where the properties, architecture, and loading of the CF predominate in the C/C composite.[3] Currently, CFs are mainly derived from polyacrylonitrile resin, petroleum pitch, and rayon. Their diameters are mainly in the range 3 to 10 μm. Their tensile strength and Young's modulus are typically 7 GPa and 1 TPa, respectively.[4] In comparison, a carbon nanotube (CNT), another member of the carbon family, has a diameter ranging from 0.4 to 50 nm, a tensile strength of 11–200 GPa, and a Young's modulus of 0.27–1.34 TPa.[5–8] Furthermore, CNTs have excellent compression properties. The compression modulus of individual multi-walled carbon nanotubes (MWCNTs) can reach 130 GPa,[9] and the compression properties of macroscopic CNTs can be used for mechanical energy storage.[10–12] Such excellent mechanical properties together with outstanding thermal[13] and electronic[13–16] properties make CNTs predicted to be the next generation of reinforcement materials.[17–19] CNTs are also believed to be excellent building blocks for C/C composites.

There are already some reports on the application of CNTs in C/C composites. However, most of them are focused on the effect of the addition of CNTs on the properties of CF-based C/C composites, and the content of CNTs in the composites is lower than 5 wt%.[20,21] Some reports investigated the synthesis and applications of CNT-based C/C composites. Chemical vapor deposition (CVD) or chemical vapor infiltration (CVI) methods and high pressure impregnation carbonization methods have been used to synthesis these composites. Allouche *et al.*[22–24] investigated the CVD of pyrolytic carbon on the surface of CNTs in detail, obtained various nanometric and micrometric morphologies, and studied the mechanism of deposition. Li *et al.*[25] produced fully densified aligned CNT films by the combination of CVD and CVI processes. The compressive modulus and electrical properties of the densified aligned CNT films increased compared to the pristine aligned CNT films. However, the alignment of the CNTs influences the anisotropism of the composites.

In this work, isotropic multi-walled CNT (MWCNT)-based C/C composites were fabricated by CVI of pyrolytic carbon into pre-compressed MWCNT blocks. The pyrolytic carbon improved the connection between the MWCNTs, building a three-dimensional network structure. After annealing at 1800 °C in vacuum, the graphitization was improved, which resulted in an

[a]*Beijing Key Laboratory of Green Chemical Reaction Engineering and Technology, Tsinghua University, Beijing, 100084, China. E-mail: wf-dce@tsinghua.edu.cn; Fax: +86-10-6277-2051; Tel: +86-10-6278-5464*

[b]*Center for Nano and Micro Mechanics, Tsinghua University, Beijing, 100084, China. E-mail: yingingzhang@tsinghua.edu.cn; Fax: +86-10-6279-8028; Tel: +86-10-6279-8503*

† Electronic supplementary information (ESI) available. See DOI: 10.1039/c3nr01069d

increase of the number of walls of the MWCNTs. The mechanical properties and electrical properties were investigated and analyzed in detail.

Experimental

Synthesis and structure of MWCNTs

The agglomerated MWCNTs, which were mass produced in a fluidized bed reactor,[26] have been used as raw materials in this study. The outer and inner diameters of the MWCNTs are ~20 nm and ~10 nm, respectively. The number of walls is ~12. The purity of the as-grown agglomerates determined by thermal gravimetric analysis is above 99%, and the apparent density is 0.04 g cm^{-3}.

Fabrication of MWCNT-based C/C composites

Fig. 1 illustrates the fabrication procedure of the MWCNT-based C/C composites. The MWCNTs were loaded into the cavity of a cylindrical die, where a punch was fixed at the top of the die. Hydrostatic pressure was applied through an oil jack. The MWCNTs were compressed at 200 MPa for 5 min to obtain a MWCNT block (denoted as P-MWCNTs). The P-MWCNTs were then placed in the quartz tube of a tube furnace. The temperature was firstly increased to 750 °C during a flow of Ar and H_2. Then, C_2H_4 and H_2 were introduced into the tube to densify the P-MWCNTs. The flow rates of Ar, H_2, and C_2H_4 were 250, 200, and 100 sccm, respectively (where sccm is standard cubic centimetres per minute). The reaction was terminated after 6 h by turning off the C_2H_4. The C/C composites were cooled down under the protection of Ar and H_2. The as-synthesized product was denoted as P-MWCNTs/C. The density of P-MWCNTs/C can be adjusted by altering the reaction time. The P-MWCNTs/C was further annealed at 1800 °C for 1 h in an electric resistance graphite oven (HZS-30). The pressure in the oven was under 10 Pa which was vacuumized from air using a multi-stage vacuum pump. The as-obtained product is denoted as A-P-MWCNTs/C. The P-MWCNTs were also treated under the same conditions for comparison and the products denoted as A-P-MWCNTs.

Characterization

The structures of the C/C composites were characterized with a JEOL JSM 7401F high-resolution scanning electron microscope (SEM) operated at 3.0 kV and a JEOL JEM 2010 high-resolution transmission electron microscope (TEM) operated at 120.0 kV. The TEM sample was prepared by a routine sonication method. Raman spectra were taken with a Renishaw Raman microprobe RM2000 with a He–Ne laser excitation line (633.0 nm) and a spot

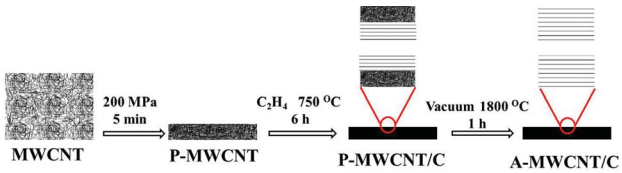

Fig. 1 Schematic of the synthesis process of MWCNT-based C/C composites.

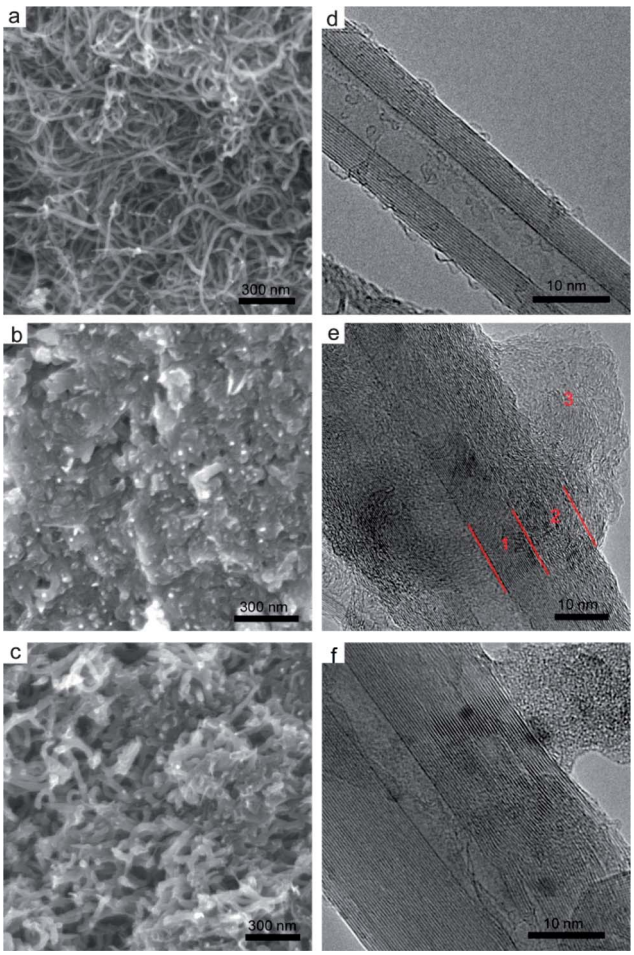

Fig. 2 (a and d) SEM and TEM images of P-MWCNT. (b and e) SEM and TEM images of P-MWCNT/C. (c and f) SEM and TEM images of A-P-MWCNT/C.

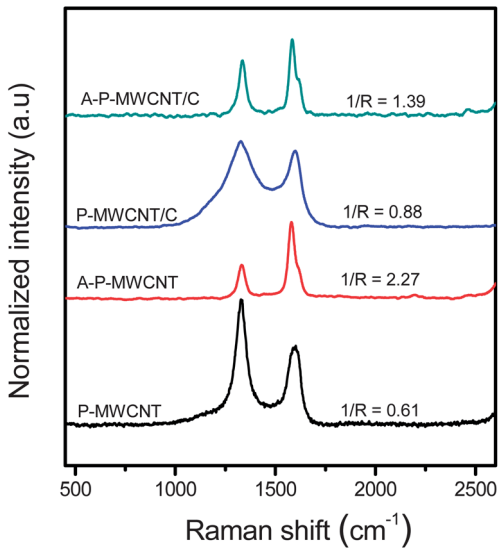

Fig. 3 Raman spectra of P-MWCNT, A-P-MWCNT, P-MWCNT/C and A-P-MWCNT/C.

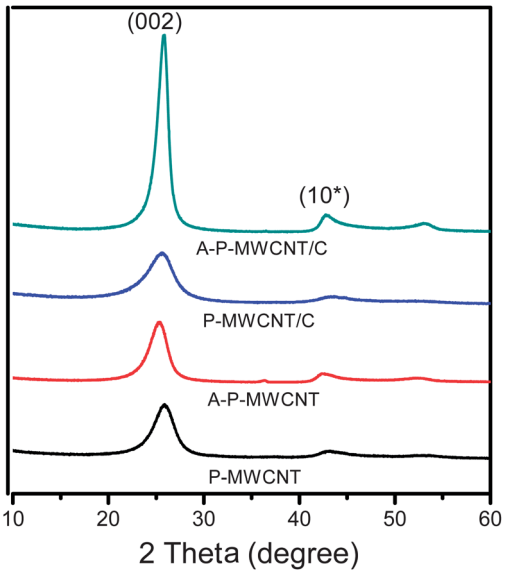

Fig. 4 XRD patterns of P-MWCNT, A-P-MWCNT, P-MWCNT/C and A-P-MWCNT/C.

Table 1 The calculated structure parameters of different samples from XRD patterns

Sample	2θ (degree)	FWHM (degree)	$d(002)$ (nm)	$L_c(002)$ (nm)	n
P-MWCNT	25.88	2.346	0.3442	3.862	11.2
A-P-MWCNT	25.32	2.073	0.3517	4.366	12.4
P-MWCNT/C	25.58	2.841	0.3481	3.188	9.2
A-P-MWCNT/C	25.89	1.302	0.3441	6.959	20.2

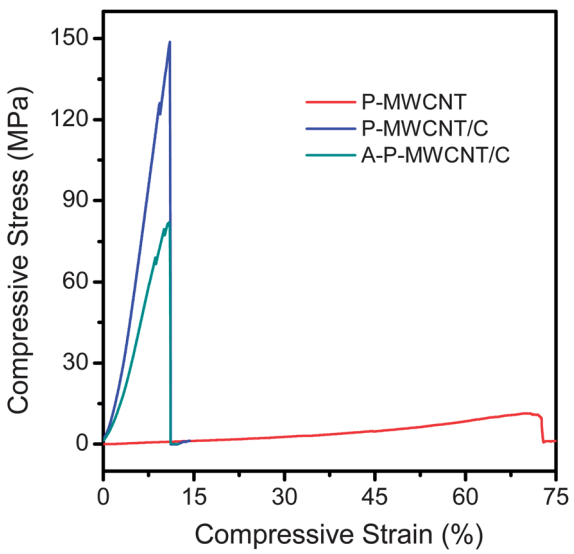

Fig. 5 Mechanical compression performance of the samples.

size of 20 μm^2. The X-ray diffraction (XRD) measurement was carried out using BRUKER XRD system with CuKα1 radiation ($\lambda = 0.15406$ nm) at a scanning velocity of 5° min^{-1}.

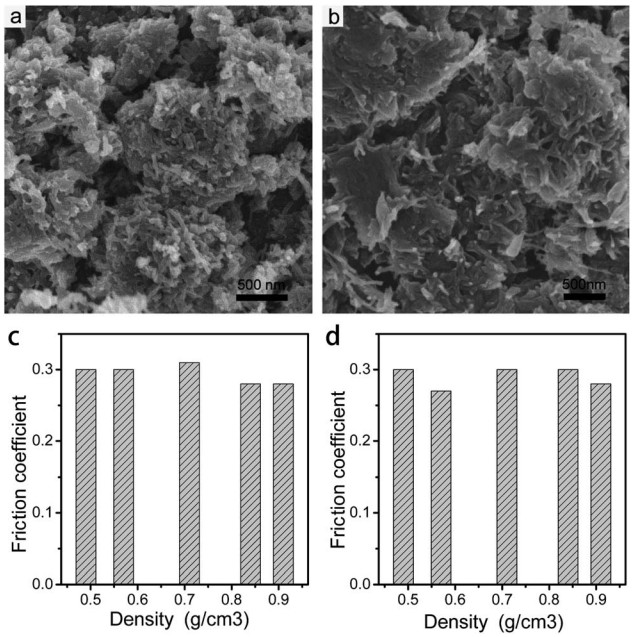

Fig. 6 (a and b) SEM images of the surface of P-MWCNT/C and A-P-MWCNT/C after tribological property testing. (c and d) Friction coefficients of P-MWCNT/C with loads of 20 N and 50 N, respectively.

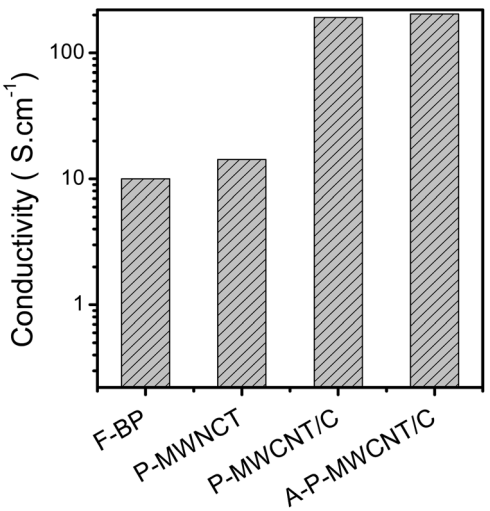

Fig. 7 Comparison of the electrical conductivity of bucky paper produced by filtration (F-BP) and our MWCNT/C composites.

Table 2 Mechanical, tribological and conducting properties of the samples

Sample	D (g cm^{-3})	σ (MPa)	ε (%)	E (MPa)	f	S (S cm^{-1})
P-MWCNT	0.28	26.2	58.7	30.1		14.3
P-MWCNT/C	1.17	148.6	10.9	1588.6	0.3	191.2
A-P-MWCNT/C	0.81	82.1	10.9	974.5	0.3	204.4

The compressive performance of the composites was measured using a ZWICK Z005 static material testing machine with a beam move speed of 1 mm s^{-1}. The size of the samples

for the compressive property testing was 55 mm × 10 mm × 4 mm, and 3–5 tests were carried out for each sample to get a reliable value. The tribological properties were tested with a SRV high temperature friction and wear tester. The load and sliding speed were fixed at 20 N or 50 N and 0.08 m s^{-1}, respectively. The electrical performance of the samples was characterized using a four-point probe resistance measurement system (KDY-1) at room temperature.

Results and discussion

The agglomerated MWCNT particles with a size ranging from 100–500 μm are three-dimensional network structures. Sub-agglomerates of about 1 μm were formed in the multi-stage agglomerates. After pressing under a hydrostatic pressure of 200 MPa, the aggregation structure of the MWCNTs was destroyed. The MWCNTs became closely packed and the characteristics of sub-agglomerates were decayed. The density (D) was measured as 0.85 g cm^{-3}. When the external force was removed, the structures recovered partially from deformation and the volume of the CNT block was expanded. The density decreased to 0.28 g cm^{-3} and the volume fraction of MWCNTs decreased to 13%. Such a CNT block can be used as a prototype for mechanical energy storage.[11]

After CVI treatment, the pyrolytic carbon was deposited on the surface of the MWCNTs and filled the gaps between the MWCNTs (Fig. 2b). The volumes of samples did not change in this process, and the density of the P-MWCNTs/C increased to 1.17 g cm^{-3}, 4 times that of the P-MWCNTs. Fig. 2e shows the TEM image of the pyrolytic carbon on the surface of the MWCNTs. Obviously, there are two kinds of configurations. Some of the pyrolytic carbon was turbostratic while other parts were disordered, which is consistent with Allouche's reports.[22–24] The turbostratic carbon was epitaxially grown on the outer walls of CNTs, while also present in the gaps between the MWCNTs, which improved the connection between the MWCNTs and formed a three-dimensional network structure. The formation of the three-dimensional network structure is expected to improve the mechanical and electrical properties significantly.

After annealing at 1800 °C in a vacuum, the density of composites decreased from 1.17 to 0.81 g cm^{-3}. This is probably due to the bulk expansion of hydrocarbon, by pyrogenation and volatilization, which was adsorbed in the composites during the process of densification. The bulk expansion is about 2%. Remarkably, annealing treatment can lead to the rearrangement of carbon and the formation of pores in the C/C composites (Fig. 2c). The turbostratic pyrolytic carbon deposited on the surface of the MWCNTs was rearranged (Fig. 2f) into graphitic carbon. And the disordered pyrolytic carbon still exists between the MWCNTs to maintain the stability of the three-dimensional network structure. The higher magnification TEM image of the connected joint of two CNTs of A-P-MWCNTs clearly revealed their mainly graphitic carbon connections (Fig. S1†).

Raman spectra have been used to characterize the graphitization degree of the C/C composites, all of them were normalized to the G+ peaks. Generally, $R = I_D/I_G$ (intensity ratio of Raman spectra D-band to G-band of MWCNTs) is used to probe the defect density of carbon materials, and $1/R$ is used to evaluate the crystal planar domain size of graphite. The higher the $1/R$ value, the better the developed graphitic structure.[27] As shown in Fig. 3, the peak at 1331 cm^{-1} (D-band) is strong, and the value of $1/R$ is 0.61 for P-MWCNTs. After annealing at 1800 °C in vacuum, the defects in the lattice of the CNTs were repaired, and the value of $1/R$ is increased to 2.27 for A-P-MWCNT. The D-band becomes wider after CVI treatment, which is attributed to the generation of turbostratic carbon.[27] With further annealing at 1800 °C in vacuum, the defects in the lattice of the CNTs were repaired, and the turbostratic pyrolytic carbon was rearranged. The $1/R$ value increased from 0.88 to 1.39, which indicates improved graphitization of A-PMWCNT/C.

The XRD patterns of P-MWCNT, A-P-MWCNT, P-MWCNT/C and A-P-MWCNT/C are shown in Fig. 4. The characteristic peaks at 25.5° and 42° are attributed to the lattice planes of (002) and (10*), respectively. According to the XRD results of carbon materials, the peak of (002) represents CNTs along the radial direction, and the peak of (10*) is the congruent of (101) and (100) peaks due to in-plane reflections. Table 1 shows the experimental and calculated results of (002) peaks of these samples. The interlayer spacing d_{002} and stack height L_c were estimated according to the Bragg equation ($d_{002} = \lambda/(2\sin\theta_{002})$) and Scherrer equation ($L_c = \lambda/(\beta\cos\theta_{002})$) respectively. Here λ, β, and θ are the wavelength of the X-ray, FWHM, and the peak position of (002) respectively. The d(002) of P-MWCNT is 0.3442 nm and L_c is 3.862 nm, which are close to the values reported in the literature.[28,29] The estimated average number of walls of the MWCNTs is 11.2, which is consistent with the result shown by TEM (Fig. 1a). After densification through CVI, the carbon deposited on the surface of the MWCNTs led to a widened (002) peak and reduced graphitization. So, the value of d_{002} and L_c cannot represent the structure of MWCNTs exactly. High temperature annealing can improve the graphitization of CNTs.[28,29] Gong *et al.*[28] proved that high-temperature treatment in an argon atmosphere could remove some in-plane defects, but could not lead to a decrease of d_{002}. However, Wu and Cheng[29] reported that d_{002} decreased and L_c increased through high-temperature treatment in an argon atmosphere. In this work, the d_{002} increased from 0.3442 nm for P-MWCNT to 0.3517 nm for A-P-MWCNT after high-temperature treatment in a vacuum. It is probable that the vacuum environment resulted in the increase of d_{002}. The L_c change of A-P-MWCNT/C can be attributed to two reasons: one is the increase of d_{002}, the other is the rearrangement and graphitizing of turbostratic carbon deposited on the surface of the MWCNTs. It is interesting that the rearrangement of turbostratic carbon took place along the axial direction of MWCNTs, which led to an increase of diameter, L_c and the number of walls of the MWCNTs. The average number of walls of the MWCNTs increased from 11.2 to 20.2, which is consistent with the images shown in Fig. 1e and f. The conversion from turbostratic carbon to CNT layers would be a good method to regulate the diameter and number of walls of MWCNTs.

Fig. 5 shows the mechanical compression performance of the samples. The deformation (ε) of P-MWCNT is dominated by the pores between the CNTs, and has a maximum deformation of 58.7%. Because of the weak van der Waals interaction between the MWCNTs, the breaking strength (σ) and Young's modulus (E) of P-MWCNT are only 26.2 and 30.1 MPa, respectively. After CVI treatment, the disordered pyrolytic carbon was deposited between the MWCNTs. The bridges between the MWCNTs were strengthened, forming a three-dimensional network structure and leading to significantly improved mechanical properties. The breaking strength and Young's modulus of P-MWCNT/C increased to 148.6 and 1588.6 MPa, respectively. Furthermore, the maximum deformation of P-MWCNT/C is 10.9% and the value of energy absorption reached 13.8 kJ kg^{-1}. This indicates that the ratio of hole compressions was reduced. Accordingly, the percentage of volume compression of MWCNTs and pyrolytic carbon were increased. After annealing at 1800 °C under vacuum, some impurities decomposed and the deposited carbon of A-P-MWCNT/C around the cross-linked pyrolytic carbon migrated accompanied by carbon rearrangement. As a result, decreased breaking strength (82.1 MPa) and Young's modulus (974.5 MPa) were detected. The break mainly comes from the destruction of structure at the cross-linking points, which has been proved by the tribological property test.

As shown in Fig. 6a and b, the top surface of P-MWCNT/C and A-P-MWCNT/C are full of spherical C/C aggregations with a diameter of *ca.* 300 nm after tribological property testing, which is similar to that of the original agglomerate MWCNTs. The friction coefficients (f) of samples with different densities or the same samples under different loads have not shown a remarkable difference (Fig. 6c and d), which indicates the cracks mainly came from the cross-linking points of the CNT agglomerates. Two conclusions can be drawn from the above results. One is that the structure of the MWCNTs is retained in the compression process, which is consistent with our previous work.[30] The other is that the weakest sites in the composites are the connection points between the MWCNTs.

The deposition curve (density *vs.* time) of Fig. S2† showed that the density of P-MWCNT/C increased with deposition time and tended to accumulate more slowly after a long deposition time (*ca.* >5 h). The morphology of P-MWCNT/C after 5 h showed a relatively uniform deposition from outside into the interior using an electron microscope technique (Fig. S3†). A longer deposition time may further improve the composite uniformity.

The electric conductivity (S) of C/C composites is very important for their broad application in the areas of aerospace and electronics. In theory, CNT has excellent electron conducting capability, the theoretical value of S can reach 10 000–30 000 S cm^{-1},[13,16] and the experimental value is 500–1250 S cm^{-1} for the individual MWCNTs produced by catalytic processes.[15] However, the reported S of CNT assemblies is much lower than that of the theoretical and measured values of individual MWCNTs, which may be due to the defects in CNTs and the high contact resistance between the CNTs. So, one of the feasible methods to increase the conductivity of CNT assemblies is to decrease the contact resistance. Fig. 7 lists typical S values of our samples. The electrical conductivity of P-MWCNTs is 14.3 S cm^{-1}, which is similar to that of bucky paper produced by filtration. After deposition of the pyrolytic carbon and annealing at high temperature, their conductivities can be improved to *ca.* 191.2 and 204.4 S cm^{-1}, respectively, an increase of more than ten times that of P-MWCNTs. This could be due to the decrease of contact resistance among sp^2 carbon agglomerates, which predominates in the total resistance. Similar to most CNT assemblies reported, there are only weak van der Waals interactions among CNTs in P-MWCNT, which means a very high contact resistance. The MWCNTs were connected by pyrolytic carbon after densification through CVI, which resulting in a decreased contact resistance and an improved conductivity. The following treatment at high temperature led to large-area sp^2 carbon domains in the C/C composites. However, the impact on the electrical connections between MWCNTs is not remarkable. Note that the mechanical, tribological and electrical conductive properties of the samples are summarized in Table 2.

Conclusions

High density and isotropic MWCNT-based C/C composites were prepared by CVI. The density of P-MWCNT/C was 1.17 g cm^{-3}, which is 4 times that of P-MWCNTs. The pyrolytic carbon improved the connection between the MWCNTs and formed a three-dimensional network structure. The graphitization of P-MWCNT/C can be significantly improved by annealing at 1800 °C in a vacuum. It is interesting to note that the diameter and the number of walls of the MWCNTs are obviously increased after the CVI and high-temperature treatment. Both the P-MWCNT/C and A-P-MWCNT/C showed excellent mechanical and electrical conducting properties. The maximum compressed deformation, breaking strength and Young's modulus of P-MWCNT/C were 10.9%, 148.6 MPa and 1588.6 MPa, respectively. The electrical conductivity of the P-MWCNT/C and A-P-MWCNT/C were 191.2 and 204.4 S cm^{-1}, respectively. These properties make MWCNT-based C/C composites promising materials for aerospace applications.

Acknowledgements

This work was supported by the National Basic Research Program of China (2011CB932602) and the National Science Foundation of China (21203107).

Notes and references

1 T. Windhorst and G. Blount, *Mater. Des.*, 1997, **18**(1), 11–15.
2 J. E. Sheehan, K. W. Buesking and B. J. Sullivan, *Annu. Rev. Mater. Sci.*, 1994, **24**, 19–44.
3 G. Dorey, *J. Phys. D: Appl. Phys.*, 1987, **20**(3), 245–256.
4 X. Huang, *Materials*, 2009, **2**(4), 2369–2403.
5 M. S. Dresselhaus, G. Dresselhaus and A. Jorio, *Annu. Rev. Mater. Res.*, 2004, **34**, 247–278.

6 M. F. Yu, *J. Eng. Mater. Technol.*, 2004, **126**(3), 271–278.
7 B. G. Demczyk, Y. M. Wang, J. Cumings, M. Hetman, W. Han, A. Zettl and R. O. Ritchie, *Mater. Sci. Eng., A*, 2002, **334**(1–2), 173–178.
8 R. Zhang, Q. Wen, W. Qian, D. S. Su, Q. Zhang and F. Wei, *Adv. Mater.*, 2011, **23**(30), 3387–3391.
9 Z. Jiong, H. Mo-Rigen, D. Sheng, H. Jia-Qi, W. Fei and Z. Jing, *Carbon*, 2011, **49**(1), 206–213.
10 A. Y. Cao, P. L. Dickrell, W. G. Sawyer, M. N. Ghasemi-Nejhad and P. M. Ajayan, *Science*, 2005, **310**(5752), 1307–1310.
11 Y. Liu, W. Qian, Q. Zhang, A. Cao, Z. Li, W. Zhou, Y. Ma and F. Wei, *Nano Lett.*, 2008, **8**(5), 1323–1327.
12 Q. Zhang, M. Zhao, Y. Liu, A. Cao, W. Qian, Y. Lu and F. Wei, *Adv. Mater.*, 2009, **21**(28), 2876–2879.
13 R. H. Baughman, A. A. Zakhidov and W. A. de Heer, *Science*, 2002, **297**(5582), 787–792.
14 H. J. Dai, *Acc. Chem. Res.*, 2002, **35**(12), 1035–1044.
15 H. J. Dai, E. W. Wong and C. M. Lieber, *Science*, 1996, **272**(5261), 523–526.
16 A. Thess, R. Lee, P. Nikolaev, H. J. Dai, P. Petit, J. Robert, C. H. Xu, Y. H. Lee, S. G. Kim, A. G. Rinzler, D. T. Colbert, G. E. Scuseria, D. Tomanek, J. E. Fischer and R. E. Smalley, *Science*, 1996, **273**(5274), 483–487.
17 J. N. Coleman, U. Khan, W. J. Blau and Y. K. Gun'ko, *Carbon*, 2006, **44**(9), 1624–1652.
18 K. Prashantha, J. Soulestin, M. F. Lacrampe and P. Krawczak, *Polym. Polym. Compos.*, 2009, **17**(4), 205–245.
19 H. Qian, E. S. Greenhalgh, M. S. P. Shaffer and A. Bismarck, *J. Mater. Chem.*, 2010, **20**(23), 4751–4762.
20 D. S. Lim, J. W. An and H. J. Lee, *Wear*, 2002, **252**(5–6), 512–517.
21 K.-J. Lee, M.-H. Hsu, H.-Z. Cheng, J. S.-C. Jang, S.-W. Lin, C.-C. Lee and S.-C. Lin, *J. Alloys Compd.*, 2009, **483**(1–2), 389–393.
22 H. Allouche, M. Monthioux and R. L. Jacobsen, *Carbon*, 2003, **41**(15), 2897–2912.
23 H. Allouche and M. Monthioux, *Carbon*, 2005, **43**(6), 1265–1278.
24 M. Monthioux, H. Allouche and R. L. Jacobsen, *Carbon*, 2006, **44**(15), 3183–3194.
25 X. Li, L. Ci, S. Kar, C. Soldano, S. J. Kilpatrick and P. M. Ajayan, *Carbon*, 2007, **45**(4), 847–851.
26 Y. Hao, Q. F. Zhang, F. Wei, W. Z. Qian and G. H. Luo, *Carbon*, 2003, **41**(14), 2855–2863.
27 M. S. Dresselhaus, G. Dresselhaus, R. Saito and A. Jorio, *Phys. Rep.*, 2005, **409**(2), 47–99.
28 Q.-M. Gong, Z. Li, Y. Wang, B. Wu, Z. Zhang and J. Liang, *Mater. Res. Bull.*, 2007, **42**(3), 474–481.
29 F. Y. Wu and H. M. Cheng, *J. Phys. D: Appl. Phys.*, 2005, **38**(24), 4302–4307.
30 Y. Liu, X. Gao, W. Qian, Y. Wang and F. Wei, *Powder Technol.*, 2011, **211**(2–3), 226–231.